Pergamon

Int. J. Heat Mass Transfer. Vol. 40, No. 15, pp. 3559–3575, 1997

Printed in Great Britain
0017–9310/97 $17.00+0.00

PII: S0017–9310(97)00001–X

Interfacial shear models and their required asymptotic form for annular/stratified film condensation flows in inclined channels and vertical pipes

A. NARAIN, GUANG YU and QINGYU LIU

Department of Mechanical Engineering–Engineering Mechanics, Michigan Technological University, Houghton, MI 49931, U.S.A.

(*Received* 8 *May* 1996 *and in final form* 5 *December* 1996)

Abstract—Internal flows of pure vapor experiencing film condensation on the bottom wall of an inclined (horizontal to vertical) channel and the inside wall of a vertical cylinder are studied. The annular flow regime considered here has turbulent (or laminar) vapor in the core and thin laminar condensate on the wall. Both smooth and wavy interfaces are considered. We propose a theory which yields a new general asymptotic form of interfacial shear, addresses solvability of the governing equations, gives the solution of the equations near the point of onset of condensation and facilitates implementation of one- or two-dimensional numerical schemes for the entire flow. The results, in a suitable limit, are shown to be in excellent agreement with a classical exact solution. We implement a one-dimensional numerical solution scheme to assess popular interfacial shear models and heat transfer correlations. These assessments, based on comparison of computational predictions with data from well-known experiments, identify two potentially good interfacial shear models which can be further developed for greater reliability. © 1997 Elsevier Science.

1. INTRODUCTION

Downward flows in inclined (horizontal to vertical) channels and vertical cylinders allow study of internal condensing flows under the influence of shear and gravity. We study these configurations (e.g. see Fig. 1) to better understand such flows, to develop one- and two-dimensional computational capabilities and to assess and propose models for interfacial shear.

The internal flows considered here are simple modifications of the classical studies dealing with external film condensation over vertical, horizontal and tilted walls. The Nusselt [1] solution for laminar and smooth film condensation of stationary vapor over a vertical wall has been improved and generalized in the works of Rohsenow [2], Sparrow and Gregg [3], Koh *et al.* [4], Chen [5], Dhir and Lienhard [6], and Sadasivan and Lienhard [7]. Heat transfer correlations for lami-

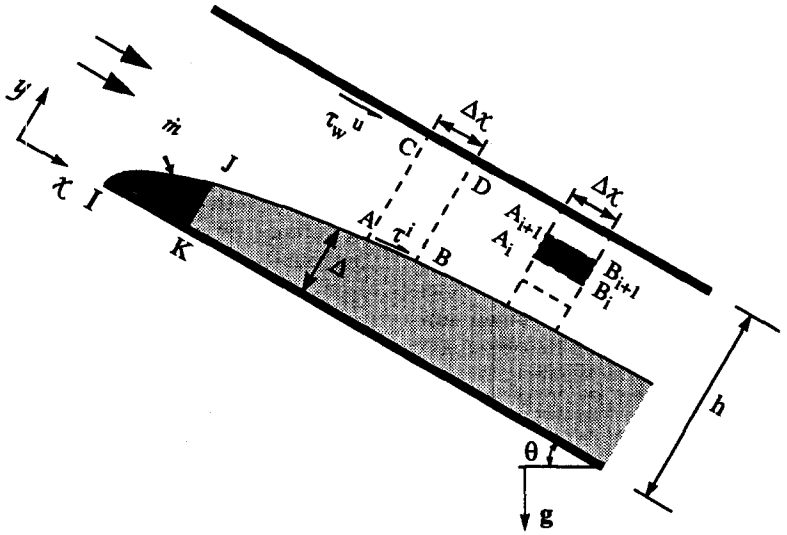

Fig. 1. The inclined channel geometry under study ($0° \leqslant \theta \leqslant 90°$).

NOMENCLATURE

Fr^{-1}	inverse Froude number, $g_x L_c/U^2$
$\mathscr{h}_{fg}$	latent heat ($\mathscr{h}_g - \mathscr{h}_f$) (J/Kg)
Ja	Jacob number, $C_{pl}\Delta\mathscr{T}/\mathscr{h}_{fg}$
L_c	duct dimensions ($L_c = h$ for channels and $L_c = D$ for pipes) (m)
$\dot{m}$	local value of physical condensation rate (kg/m^2 – s)
$\dot{m}$	non-dimensional value of local condensation rate
p	physical pressure (N/m^2)
p_o	pressure at the inlet (N/m^2)
Re_1	Reynolds number $\rho_1 U L_c/\mu_1$, $I = 1$ or 2
Re_L	liquid Reynolds number defined in (A5)
(u, v)	values of x and y components of physical velocity (m/s)
(u, v)	non-dimensional u and v
u_f	non-dimensional value of the speed at the interface
U	physical value of the average vapor speed at the inlet (m/s).

Greek symbols

Δ	physical value of condensate thickness (m)
δ	non-dimensional value of Δ.

Subscripts

1	liquid
2	vapor
w	wall.

Superscripts

i	interface location.

nar and wavy condensate are given in Kutateladze [8] and correlations for turbulent condensate have been proposed by Labuntsov [9]. Experimental results for the vertical wall geometry have been documented by Gregorig *et al.* [10]. Film condensation on vertical walls under combined effects of forced convection and gravity has been studied by Fujii and Uehara [11]. Shear driven laminar condensation flow over a horizontal plate has been studied by Cess [12], Koh *et al.* [4], Koh [13], etc. However, these works for the horizontal configuration do not deal with flow regimes involving wavy condensate or turbulent vapor.

Annular film condensation for downflow in a vertical tube has been studied by analytical/computational means, under various simplifications and assumptions, in the works of Shekriladze and Mestvirishvilli [14], Dobran and Thorsen [15], Wang and Tu [16], etc. Experimental studies or heat transfer correlations for this flow can be found in the works of Carpenter and Colburn [17], Goodykoontz and Dorsch [18], Cavallini and Zecchin [19], Shah [20], etc.

In the presence of waves, development of good models for mean interfacial shear acting on the mean location of the interface is important because of its necessity in any meaningful theoretical (or computational) prediction capability. Such modeling could, in future, be related to relevant information obtained from an understanding of the complex interaction of turbulent gas flows over wavy liquid flows or wavy walls. A wavy interface can be viewed as a surface endowed with oscillatory roughness elements placed in a suitable spatial arrangement with prescribed spatio-temporal variations in amplitude, phase, and frequency. Significant issues for wavy gas liquid flows are discussed in Dukler [21], Dukler [22], Hanratty [23], etc. Detailed wave structure studies for gas/liquid flows or full two-dimensional numerical simulations can provide insight on flow fields (recirculating gas flow in the wake of a liquid crest, recirculating flow in the liquid crest itself, etc.) and an understanding of the pressure drag and skin friction contributions to the mean value of interfacial shear. However, this paper limits itself to the development of interfacial shear models by a traditional approach, e.g. wall shear modeling of Moody [24] for pipe flows, etc. A traditional approach merely requires that first principle based theory employing the interfacial shear model (this being the only tentative input to the theoretical analysis) should predict mean flow variables in reasonable agreement with experimental measurements.

Extending the work of Narain [25] for condensing flows in a horizontal channel, a much simpler argument is given in this paper to establish a more general and universal asymptotic form of interfacial shear at the point of onset of condensation ($\chi = 0$)—a point of mathematical singularity where film thickness is conveniently known to be zero and condensation rate is infinite. The new form of asymptotic model proposed here allows us to resolve the elliptic singularity (see Sections 3 and 5) at $\chi = 0$. The resolution of singularity, with the help of a computer algebra based algorithm, provides an explicit analytical/computational solution at $\chi \sim 0$. We show that this algorithm, in a suitable limit, predicts numerical results in excellent agreement with the classical exact similarity solutions of Cess [12], Koh [13], etc. for laminar/laminar film condensation flows over a horizontal plate. For the gravity assisted flows in tilted channels ($0° < \theta \leqslant 90°$ in Fig. 1) or vertical cylinders, we only consider shear dominated flow regimes at $\chi \sim 0$. As a result of shear dominance, film thickness variation at $\chi \sim 0$ is $\Delta(\chi) \sim \chi^{1/2}$. The limiting analysis for the gravity dominated flow regime at $\chi \sim 0$ and

interesting demarcation of the parameter space into shear dominated ($\tau^i \gg \rho_1 g_x \Delta$) and gravity dominated ($\tau^i \ll \rho_1 g_x \Delta$) regimes are important (see Chen *et al.* [27]) and will be addressed in a forthcoming paper. For example, for the flow in Fig. 1, at $\theta = 90°$, large gaps h, and small values of U, the proposed analysis for vertical channels can be modified to yield predictions in agreement with the Nusselt [1] result: $\Delta(\chi) \sim \chi^{1/4}$ at $\chi \sim 0$.

The one-dimensional numerical solution scheme developed and employed here is adequate for assessment of popular interfacial shear models. For this, we compare numerical predictions for any given interfacial shear model with data from the following experiments: (i) downflow steam condensation in a vertical tube, Goodykoontz and Dorsch [18]; (ii) downflow R11 vapor condensation in a vertical tube, Cavallini and Zecchin [19]; and (iii) R113 vapor condensation on the bottom plate of a rectangular duct, Lu [28] and Lu and Suryanarayana [29].

Currently we do not have sufficiently general flow regime maps to predict, at the outset, whether the flow being considered, corresponds to a negligible entrainment annular flow or not. It should be noted that various other gas/liquid configurations (annular with entrainment, slug, plug, etc.) are possible. However, because vapor fraction is 100% at the inlet of the duct, up to a certain inlet mass flux of dry vapor, a certain temperature difference $\Delta\mathscr{T}$ between the vapor and the condensing surface, and a certain length L of the channel—stable annular film condensation flows (with or without interfacial waves under negligible entrainment) are expected. This fact, along with direct visual observation (when available) of experimental runs, trends in experimental data, trends in computational predictions and flow regime maps of Bell *et al.* [30], Palen *et al.* [31], etc. has been used by us to infer whether a flow is annular (with negligible entrainment effects) or not.

The following relevant and representative interfacial shear models have been assessed: (i) friction factor models as if the gas was flowing over an impermeable wall (as in Soliman *et al.* [32]); (ii) Shekriladze and Gomelauri [26] model; (iii) Mickley [33] or Film Models (see p. 599 of [34]); (iv) Henstock and Hanratty [35] and related Andreussi model [36]; (v) Narain [25] model as a generalization of Spedding and Hand [37] type model; and (vi) Wallis [38] model. We identify that a modified Henstock and Hanratty/Andreussi model or Narain [25] type model are "good" models deserving further development.

A good interfacial shear model predicts the flow variables correctly and, therefore, allows consistent assessment of different heat transfer coefficients. In this spirit, we assess, in a limited range, some heat transfer coefficients of Traviss *et al.* [39], Shah [20] and Numrich [40] for the vertical tube geometry.

2. NON-DIMENSIONAL PARAMETERS AND MODEL EQUATIONS FOR FLOW IN AN INCLINED CHANNEL

We denote the liquid and vapor phases in the flow (e.g. see Fig. 1) by a subscript I: $I = 1$ for liquid and $I = 2$ for vapor. The fluid properties (density ρ, viscosity μ, specific heat C_p and thermal conductivity k) with subscript I are assumed to take their representative constant values for each phase ($I = 1$ or 2). Let $\mathscr{T}_I$ be the mean temperature fields, p_I be the mean pressure fields, $\mathscr{T}_s(p)$ be the saturation temperature of the vapor as a function of the pressure p, Δ be the mean film thickness, $\dot{m}$ be the local interfacial mass transfer rate per unit area, $\mathscr{T}_w(\chi)$* ($< \mathscr{T}_s(p)$) be a known temperature variation of the bottom plate and $\mathbf{v}_I = u_I\mathbf{i} + v_I\mathbf{j}$ be the mean steady velocity fields. The distinction between mean and actual flow variables vanishes for smooth interface laminar flows. Furthermore, let L_c be a characteristic length for the flow, g_x and g_y be the components of gravity along x and y axes, p_0 be the inlet pressure, $\Delta\mathscr{T} \equiv \mathscr{T}_s(p_0) - \mathscr{T}_w(0)$ be the controlling temperature difference between the vapor and the bottom plate, $h_{fg}^{\circ} \equiv h_g - h_f$ be the latent heat of vaporization at the inlet temperature $\mathscr{T}_s(p_0)$, and U be the average inlet vapor speed determined by the inlet mass flux. With (χ, y) representing physical distances of a point with respect to the axes ($\chi = 0$ is at the inlet and $y = 0$ is at the condensing surface), we non-dimensionalize the variables as

$$\{\chi, y, \Delta, u_I, \dot{m}\} \equiv \{L_c x, L_c y, L_c \delta, U u_I, \rho_1 U \dot{m}\}$$

$$\{v_1, \mathscr{T}_1, p_1\} \equiv \{U v_I, (\Delta\mathscr{T})T_I, p_0 + \rho_I U^2 \pi_I\}. \quad (1)$$

For channel flows (see Fig. 1), $L_c = h$. For downflows in a pipe of diameter D, the characteristic distance $L_c = D$ and the radial location r ($0 \leqslant r \leqslant D/2$) of a point is replaced by the corresponding radial distance y ($y \equiv D/2 - r$) from the wall.

The scaled differential forms of mass, momentum (x and y components) and energy equations for the interior of either of the phases, the interface conditions, the conditions at the condensing surface ($y = 0$) or upper wall ($y = 1$) are well-known and can be found in Carey [41] or Narain [42]. An inspection of these equations yield the fact, that, for thin films and fixed acceleration due to gravity, the flow is affected by the following minimal set of five independent non-dimensional parameters:

$$\left\{Re_{in}, \frac{Ja}{Pr_1}, Fr^{-1}, \frac{\rho_2}{\rho_1}, \frac{\mu_2}{\mu_1}\right\}, \quad (2)$$

where $Re_{in} \equiv \rho_2 U L_c/\mu_2 \equiv Re_2$, $Pr_1 \equiv \mu_1 C_{p1}/k_1$,

* The wall temperature $\mathscr{T}_w(\chi)$ is considered experimentally known. However, if appropriate information is available, $\mathscr{T}_w(\chi)$ can be assumed and the correct value can be iteratively obtained by solving the conjugate problem dealing with conduction in the adjacent plate and convection to the coolant flowing underneath.

$Ja \equiv C_{pl}\Delta\mathscr{T}/\mathscr{H}_{fg}^{\circ}$ and $Fr^{-1} \equiv g_x L_c/U^2$. Here Re_{in}, Fr^{-1} and Ja/Pr_l are control parameters associated with inlet speed U, inclination θ and temperature difference $\Delta\mathscr{T}$. The density ratio ρ_2/ρ_1 and viscosity ratio μ_2/μ_1 are passive fluid parameters. However, when the interface is wavy, the equations governing the evolution of superposed disturbances imply additional dependence on the surface tension parameter ($\sigma/\rho_1 U^2 L_c$, or equivalently, $\sigma\rho_1 L_c/\mu_1^2$, where σ is the liquid/vapor surface tension) and another gravity parameter ($g_y L_c/U^2$ or the tilt angle θ in Fig. 1). The surface tension and the normal component of gravity (g_y) play a role in determining the critical inlet Reynolds number Re_{LL} at which two dimensional waves first appear on the smooth interface at some downstream location. In other words, for any fixed orientation with respect to gravity, the surface tension parameter (say $\sigma\rho_1 L_c/\mu_1^2$) should be added to the argument list for Re_{LL} (termed Re_L in Ref. [25]) in equation (28) of Narain [25]. However, once the interface is fully rough (i.e. $Re_{in} > Re_U$, where Re_U, as in equation (28) of [25], is the inlet Reynolds number at which three-dimensional waves fully cover the interface), the surface tension forces become unimportant in comparison to the pressure and friction drag on the oscillating roughness elements (the waves). In the fully rough regime, the surface tension effects are perhaps only responsible for wrinkles on the more dominant modest curvature shear/gravity/inertia waves (roll waves, etc.). The above description of the role of surface tension is in accord with known results for water films flowing down an incline (see p. 8 of Alekseenko *et al.* [43] for $\theta < 90°$). Therefore, excluding an often narrow parameter zone of $Re_{LL} \leqslant Re_{in} \leqslant Re_U$, for fluids and flow speeds considered here, wave effects are adequately accounted for by the inlet Reynolds number Re_{in}, the non-dimensional temperature difference Ja/Pr_l, and the inverse Froude Number Fr^{-1}. For the vertical configuration, Re_{LL} is small and Re_U is the demarcation (see Andreussi [36]) between rippled interface regime and larger amplitude disturbance wave regime. However, in the vertical configuration, as we see later, much of the rippled interface regime $Re_{LL} \leqslant Re_{in} \leqslant Re_U$ is nearly smooth in the sense that the ripples do not have a significant impact on f_{rel} (defined in equation (3) below).

For laminar or turbulent flows of vapor, the one-dimensional approach only needs the values of the vapor shear at the interface ($y = \delta(x)$) and at the upper wall ($y = 1$). For these stresses, shown in Fig. 1, we define the friction factors f, f_{rel} and f_u through the relations

$$\tau^i(x) \equiv \frac{1}{2}\rho_2(Uu_{av}(x))^2 f \equiv \frac{1}{2}\rho_2\{U(u_{av}(x) - u_i(x))\}^2 f_{rel}$$

$$\tau_w^u(x) \equiv \frac{1}{2}\rho_2(Uu_{av}(x))^2 f_u, \qquad (3)$$

where inlet speed U and the non-dimensional average speed $u_{av}(x)$ are given by

$$U \equiv \frac{1}{h}\int_0^h u_2(0, y)\mathrm{d}y,$$

$$u_{av}(x) \equiv \frac{1}{1-\delta(x)}\int_{\delta(x)}^1 u_2(x, y)\mathrm{d}y \qquad (4)$$

and $u_i(x) \equiv u_2(x, \delta(x)) \approx u_1(x, \delta(x))$ is the non-dimensional value of fluid speed at the interface.

Further approximations for thin film flows

These approximations are the same as in Narain [25]. Therefore, equation (6) of Narain [25] continues to define the linear liquid temperature profile while the liquid velocity profile in equation (5) of Narain [25] is replaced by

$$u_1(x, y) = \frac{\mu_2}{\mu_1} Re_{in}\left[\left(-\frac{\mathrm{d}\pi}{\mathrm{d}x} + Fr^{-1}\frac{\rho_1}{\rho_2}\right) \times y\left(\delta(x) - \frac{y}{2}\right) + \frac{y}{2}u_{av}^2(x) f\right]. \qquad (5)$$

The additional Fr^{-1} term above accounts for gravity assistance available in the tilted channel and vertical pipe configurations.

The non-dimensional governing equations for the one-dimensional approach

For the tilted channel flow in Fig. 1, the governing equations are the overall mass balance, interface energy balance, and vapor momentum balance. These are, respectively, given by equations (7)–(9) of Narain [25]. For the vertical tube, the corresponding equations are similarly obtained.

3. A HEURISTIC ARGUMENT FOR ASYMPTOTIC SHEAR

The classical equations (see Koh [13], Narain [42], etc.) for annular film condensation are based on standard scaling approximations (Chen and Kocamustafaogullari [44], etc.) valid only for $\chi \geqslant \varepsilon$ for some small $\varepsilon > 0$. Loosely speaking, these equations are parabolic in x-direction and elliptic in y-direction. This means that inlet conditions (including $\Delta(0) = 0$) at $\chi = 0$, the bottom wall conditions at $y = 0$, the interface conditions at $y = \Delta(\chi)$, and the top wall conditions at $y = h$ should suffice for their solution. However, unlike classical boundary layer equations for a single fluid flow, the situation here is complicated by the fact that the singularity at $\chi = 0$ requires, for a solution, a certain asymptotic behavior of interfacial shear τ^i and this makes the behavior of the equations "elliptic" over $0 \leqslant \chi \leqslant \varepsilon$. By "elliptic" we mean that the information at $\chi = 0$ is not sufficient, one has to depend on information from $\chi > 0$ to predict the solution at $\chi \sim 0$. The scaling assumptions fail at $\chi \sim 0$ because $\mathrm{d}\Delta/\mathrm{d}\chi$, curvature, etc. are large, and interfacial shear τ^i is not nearly parallel to χ-axis. In fact the governing equations studied in this paper or,

for that matter, in the classical papers of Nusselt [1], Koh *et al.* [4] etc. do not even model the flow physics over $0 \leqslant \chi \leqslant \varepsilon$. Therefore the purpose of resolving the singularity over this region is to obtain "that" significant information which is required for a valid connection between the known inlet conditions at $\chi = 0$ and the solution of the valid governing equations over $\chi \geqslant \varepsilon$. In order to use the classical formulation and the convenient inlet condition $\Delta(0) = 0$, we can extend the scaling to an inlet region $0 \leqslant \chi \leqslant \varepsilon$ provided we understand the above stated purpose. Since, at $\chi \sim 0$, liquid condensate is laminar and very thin (no inertia) condensation rate per unit area $\dot{m}(\approx k_1 \Delta \mathscr{T}/h_{fg}^{\circ}\Delta)$ becomes high and this makes the interfacial shear (due to large $\partial v_2/\partial\chi$ term) very large. However for compatibility with $\chi \geqslant \varepsilon$, it is reasonable to assume a shear dominated ($\tau^i \gg \rho_1 g_x \Delta$) inertia free region for the thin condensate at $\chi \sim 0$. The flow, primarily driven forward by interfacial shear τ^i, is given by

$$u_1(\chi, y) \sim \frac{\tau^i(\chi)}{\mu_1} y \tag{6}$$

for $\chi \sim 0$. Requirement of mass balance for the tiny leading edge control volume IJK in Fig. 1 gives

$$\int_0^{\chi} \dot{m}(\chi)\mathrm{d}\chi = \rho_1 \int_0^{\Delta(\chi)} u_1 \mathrm{d}y. \tag{7}$$

On substitution of equation (6) in equation (7), we find that the asymptotic (at $\chi \sim 0$) form of interfacial shear $\tau^i(\chi)$ is given by

$$\tau^i(\chi) \approx \frac{2\nu_1}{\Delta^2} \int_0^{\chi} \dot{m}(\chi)\mathrm{d}\chi. \tag{8}$$

Since the above integral in equation (8) requires information from a "neighbourhood" of $\chi = 0$ (and not just $\chi = 0$), we have termed the singularity at $\chi = 0$ "elliptic". Under the non-dimensionalization notations in equations (1)–(3), equation (8) becomes

$$f_{asy} \equiv f|_{x\to 0} \approx \frac{4}{Re_1 \delta^2(x)} \left(\frac{\rho_1}{\rho_2}\right) \int_0^x \dot{m}\,\mathrm{d}x, \tag{9}$$

where from equations (6) and (8) or Narain [25], $\dot{m} \approx (Ja/Pr_1)(1/Re_1)(1/\delta)$. In Section 5 of this paper, we formally show that equation (8), despite the heuristic nature of the above arguments, remains the required asymptotic form even in the presence of all the other constraints imposed by vapor momentum balance; interface mass, momentum, and energy transfer rates; and presence of other forces contributing to the motion of the condensate.

However, for certain vertical or tilted flow situations under low (or zero) vapor speeds U (large Fr^{-1}), gravity is significant ($\tau^i \sim \rho_1 g_x \Delta$) or gravity dominates ($\rho_1 g_x \Delta \gg \tau^i$) at $\chi \sim 0$. In this situation, gravity contribution on the right side of equation (6) becomes significant over a control volume IJK in Fig. 1. Therefore, for such situations, equations (6) and (8) need to be modified.

Note that substitution of equation (5) of this paper and equations (6) and (8) of Narain [25] into the mass balance equation (7) of Narain [25] gives, for the flow in Fig. 1, the expression:

$$f = \left[\{1 - u_{av}(1-\delta)\} \frac{4}{Re_1 u_{av}^2 \delta^2} - \frac{4}{3}\frac{\rho_1}{\rho_2}\frac{Fr^{-1}}{u_{av}^2}\delta + \frac{4}{3}\frac{\mathrm{d}\pi}{\mathrm{d}x}\frac{1}{u_{av}^2}\delta \right]. \tag{10}$$

The first term in equation (10) is dominant over the control volume IJK in Fig. 1 for flow situations involving small to moderate Fr^{-1} (horizontal and some gravity assisted situations) and this leads to equation (9). For large Fr^{-1} (e.g. stagnant vapor condensing on vertical walls), the first two terms of equation (10) are dominant over most of the control volume IJK in Fig. 1.

4. THE CLASSICAL ONE-DIMENSIONAL FORMULATION

We assume that the condensate flow is laminar and thin. Next we make a choice of uniform (as in equation (10) of Narain [25]) vapor velocity profile. For flows considered here, relevant results for the horizontal case described in Section 3 of Narain [25] apply. For the flow in Fig. 1, the governing equations described earlier are cast in the form of equation (12) of Narain [25] and then recast in an equivalent form

$$\frac{\mathrm{d}\mathbf{y}}{\mathrm{d}x} = \mathbf{g}(\mathbf{y}, f), \quad f = f\left(x, Re_{in}, Fr^{-1}, \frac{Ja}{Pr_1}, \frac{\rho_2}{\rho_1}, \frac{\mu_2}{\mu_1}\right),$$
$$\mathbf{y}(0) = [0, 1, 0]^T, \tag{11}$$

where $\mathbf{y} \equiv [\pi(x), u_{av}(x), \delta(x)]^T$, $\mathbf{g} \equiv [g_1, g_2, g_3]^T$ and components g_1, g_2 and g_3 of $\mathbf{g}$ are written in terms of A_{22}, A_{23}, A_{32} A_{33}, b_1, b_2 and b_3 appearing in the intermediate equation form specified by equation (12) of Narain [25].

For downflow in tilted channels, except for a corrected definition of A_{22} and a new definition of b_1 given by equations (A1)–(A2) in the Appendix of this paper, the rest of the terms appearing in the definition of g_1, g_2 and g_3 in equation (11) above are the same as those given by equations (A1)–(A11) in the Appendix of Narain [25]. In the above formulation, f_u defined in equation (3) is assumed to be given by f_0 defined in equation (13) of Narain [25]. For downflow in vertical pipes, the definitions of A_{22}, A_{32}, A_{33}, b_1 and b_3 change from the above specification of g_1, g_2 and g_3 for the tilted channel case. These new definitions are easily obtained and will be reported elsewhere.

5. FORMAL RESULTS ON THE SOLVABILITY OF THE EQUATIONS AND THE RESOLUTION OF THE SINGULARITY

The requirement $\delta(0) = 0$ makes the function $\mathbf{g}$ in equation (11) singular. Trial and error method of

guessing an initial condition at a small $x = \varepsilon$ was found to have an extremely low success rate because the solution does not exist for just any f. Therefore, one has to guess a consistent set of four values, namely: δ, u_{av}, f and π at $x = \varepsilon$. By consistent, it is meant that all balance laws are satisfied for control volumes having edges at $x = 0$ and $x = \varepsilon$. Furthermore, because of non-uniqueness of such consistent sets of values, not all consistent guesses may work! Clearly a methodical resolution of singularity is needed. An investigation of equation (11) for the flow in Fig. 1, with the help of modern computer algebra, establishes the following result.

Theorem

There exists a solution of equation (11) if and only if the friction factor is of the form

$$\begin{aligned} f &= \frac{4}{Re_1}\left\{\frac{c_1+c_2}{c_1^2}\right\}\frac{1}{x^{1/2}}+0(1) \\ &= \frac{4}{Re_1}\left\{\frac{1-u_{av}(1-\delta)}{u_{av}^2\delta^2}\right\}+0(1) \\ &= \frac{4}{Re_1}\left(\frac{\rho_1}{\rho_2}\right)\frac{1}{\delta^2}\int_0^x \dot{m}\,dx+0(1) \\ &= \frac{8}{Re_1^2}\left\{\frac{Ja}{Pr_1}\frac{\rho_1}{\rho_2}\right\}\frac{1}{c_1^3x^{1/2}}+0(1) \end{aligned} \tag{12}$$

where the constants c_1 and c_2 appear in the definition of the vector $\mathbf{y}_1$ appearing in the asymptotic solution:

$$\mathbf{y}(x) = \mathbf{y}_0+\mathbf{y}_1x^{1/2}+\mathbf{y}_2x+\mathbf{y}_3x^{3/2}+O(x^{3/2}). \tag{13}$$

In equation (13) above, $\mathbf{y}_0 \equiv \mathbf{y}(0) = [0, 1, 0]^T$, $\mathbf{y}_1 \equiv [k_1, -c_2, c_1]^T$, $\mathbf{y}_2$ and $\mathbf{y}_3$ are constant vectors. The numbers k_1 and c_2 and the vectors $\mathbf{y}_2$, $\mathbf{y}_3$, etc. are known when c_1 is known. For example, for tilted channels, k_1 and c_2 continue to be given by equations (A12) and (A13) in the Appendix of Narain [25] and for vertical pipes, they are obtained by a similar procedure.

The constant c_1 is obtained as a convergent root among the zeroes of a sequence of well defined nonlinear functions $\Psi^{(N)}$. The steps needed for generating the complex definitions of $\Psi^{(N)}$, $\mathbf{y}_2$, $\mathbf{y}_3$, etc. on the computer are the same as that described in Section 5 of Narain [25]. The functions $\Psi^{(N)}$ are of the form

$$\Psi^{(N)}\left(c_1, Re_{in}, \frac{Ja}{Pr_1}, Fr^{-1}, \frac{\rho_2}{\rho_1}, \frac{\mu_2}{\mu_1}\right) = 0 \tag{14}$$

where $N = 1, 2, 3, \ldots$, is a positive integer. For tilted channel flows, we restrict the parameters in (2) to the useful range:

$$\begin{aligned} &0.004 \leqslant \frac{\rho_2}{\rho_1} \leqslant 0.009,\ 0.016 \leqslant \frac{\mu_2}{\mu_1} \leqslant 0.026, \\ &0.009 \leqslant \frac{Ja}{Pr_1} \leqslant 0.045, \\ &9500 \leqslant Re_{in} \leqslant 90\,000 \quad \text{and} \quad 0 \leqslant Fr^{-1} \leqslant 0.7. \end{aligned} \tag{15}$$

We write the numerically obtained convergent root of equation (14) in the convenient form:

$$c_1 \equiv c_{10}+\Delta c_1 \tag{16}$$

where c_{10} is the root of equation (14) for $Fr^{-1} = 0$ and c_1 is the root of equation (14) for $Fr^{-1} \neq 0$.

For downflow in channels, under the assumption of uniform vapor velocity profile, numerically obtained convergent root of equation (14) is given, for the parameter range specified in equation (15), by the approximate power law fit:

$$\begin{aligned} c_{10} &= 1.1845\left(\frac{\rho_2}{\rho_1}\right)^{0.1113}\left(\frac{\mu_2}{\mu_1}\right)^{-0.3683}\left(\frac{Ja}{Pr_1}\right)^{0.2442} \\ &\quad\times (Re_{in})^{-0.4022} \\ \Delta c_1 &= 0.7861\left(\frac{\rho_2}{\rho_1}\right)^{-0.0432}\left(\frac{\mu_2}{\mu_1}\right)^{-0.3225}\left(\frac{Ja}{Pr_1}\right)^{0.1443} \\ &\quad\times (Re_{in})^{-0.3097}(Fr^{-1})^{0.2281}. \end{aligned} \tag{17}$$

For downflow in pipes, equations (12), (15) and (17) are suitably modified. In this case, convergent root of equation (14) is given, for the parameter range specified in equation (15), by the approximate power law fit:

$$\begin{aligned} c_{10} &= 0.9898\left(\frac{\rho_2}{\rho_1}\right)^{-0.1651}\left(\frac{\mu_2}{\mu_1}\right)^{-0.4865}\left(\frac{Ja}{Pr_1}\right)^{0.5941} \\ &\quad\times (Re_{in})^{-0.4937}, \\ \Delta c_1 &= 0.6468\left(\frac{\rho_2}{\rho_1}\right)^{0.02876}\left(\frac{\mu_2}{\mu_1}\right)^{-0.3121}\left(\frac{Ja}{Pr_1}\right)^{0.1161} \\ &\quad\times (Re_{in})^{-0.3074}(Fr^{-1})^{0.1927}. \end{aligned} \tag{18}$$

In the parameter space (2), over the hyper square in equation (15), the solution in equations (17) or (18) of equation (14) models a hyper plane "close" to the solution surface $c_1 = c_1(Re_{in}, Ja/Pr_1, Fr^{-1}, \rho_2/\rho_1, \mu_2/\mu_1)$ represented under a logarithmic scale for c_1 and all its arguments. Note that for any power law correlation, over a hyper square (such as equation (15)), the exponents of parameters on the right side of equations (17)–(18) may not be representative near the edges of the hyper square. This is because, different adjacent hyper squares can be chosen to cover the same data points at the boundary and, over different hyper squares, one may need hyper planes of quite different orientations to fit more drastic bends in the adjacent portions of the same solution surface. Therefore, more important than the exponents is the fact that the fits given by equations (17)–(18), over (15), are within $\pm 7\%$ of the convergent roots obtained directly by numerical solution (by bisection method) of equation (14).

Table 1. Numerical verification of equation (20) for the limiting situation of flow over a horizontal plate ($Fr^{-1} = 0$)

Flow situation	Re_{in}	Converged c_1 from $\Psi^{(N)} = 0$ $N = 2, 3.$ (method of Section 5)	η_δ method of Koh [13]	$\sqrt{(\rho_1\mu_2)/(\rho_2\mu_1)}c_1\sqrt{Re_{in}}$ (method of Section 5)	$f_2''(0)$ (from f_2' in method of Koh [13])	$(1/2)f(x)\sqrt{xRe_{in}}$ (2 and 3 term expansions by the method of Section 5)	
						x = 10^{-5}	x = 0.005
Case I	625	1.03102		1.592		0.65123	0.65124
$\rho_2/\rho_1 = 0.00495$	10^4	0.0075	1.5921	1.592	0.65109	0.65123	0.65124
$\mu_2/\mu_1 = 0.02087$	15×10^4	0.00200		1.592		0.65123	0.65124
$Ja/Pr_1 = 0.00668$	19×10^4	0.00178		$1.592 \approx \eta_\delta$		$0.65123 \approx f_2''(0)$	$0.65124 \approx f_2''(0)$
Case II	625	0.04862		1.462		0.53742	0.53742
$\rho_2/\rho_1 = 0.05266$	10^4	0.01215	1.4619	1.462	0.53746	0.53742	0.53742
$\mu_2/\mu_1 = 0.07620$	15×10^4	0.00314		1.462		0.53742	0.53742
$Ja/Pr_1 = 0.02659$	19×10^4	0.00279		$1.462 \approx \eta_\delta$		$0.53742 \approx f_2''(0)$	$0.53742 \approx f_2''(0)$

Proof of the theorem/results on non-uniqueness

With appropriate modifications, the proof and other results are similar to those in Section 6 of Narain [25]. Furthermore, the numerically obtained c_1 values have trends similar to that shown in Table 1 of Narain [25]. Therefore, there is non-uniqueness if we are only looking for a consistent set of values of δ, u_{av}, π and f at some $x = \varepsilon$. However, the stable solution corresponding to a convergent root should satisfy the asymptotic shear requirement in equation (12) for any small $x \sim 0$. This condition is met only by that root of equation (14) which is independent, or nearly independent, of N in $\Psi^{(N)}$. The stable root, thus chosen, leads to the determination of the constant vectors $\mathbf{y}_1$, $\mathbf{y}_2$, $\mathbf{y}_3$, etc. and these vectors bring information from the downstream regions towards the resolution of the elliptic singularity at $x \sim 0$.

Dependence of c_1 *on velocity profile and* f *at large* x

If we choose a non-uniform velocity profile in the formulation leading to equation (11), a convergent root for c_1 is obtained which is generally different from the values in equations (17)–(18). This is understandable because the interfacial shear should depend, in laminar or turbulent flows, on the nature of vapor velocity profile. Despite this, the solution of this classical one-dimensional problem in equation (11) is very useful because it can be used for subsequent two-dimensional numerical solution (e.g. by employing tiny finite volume elements shown in Fig. 1). In the two-dimensional simulation, iterative improvements of δ, u_{av} (through equation (4)), and asymptotic shear (as given by the convenient form on the right side of the second equality in equation (12)) would lead to the needed resolution of singularity at $x \sim 0$ and a converged solution of δ, f and u_2 (x, y) for $x \geqslant \varepsilon$. In this paper, a two-dimensional solution is not obtained. Yet, the results in equations (12)–(18) provide a valuable one dimensional numerical integration tool (see Section 7) for obtaining a good solution of the problem at large x with the help of a "good" model for f at large x.

Limits imposed by vapor speed and gap size for tilted configurations $\mathrm{Fr}^{-1} \neq 0$

For the flows considered here, we find that the root of c_1 of $\Psi^{(N)}$ in equation (14) does not converge for large values of Fr^{-1}. Hence, asymptotic solution in the form of equation (13) is possible only for Fr^{-1} in a restricted shear dominated range (such as equation (15)). For large Fr^{-1}, one should replace the asymptotic shear in equation (9) by the first two terms in equation (10). When this is done and a suitable analysis is performed, one can obtain, as we show in a forthcoming paper, the limiting Nusselt [1] solution behavior of $\delta(x) \sim x^{1/4}$ at $x \sim 0$.

6. COMPATIBILITY OF THE NEW THEORY WITH THE KNOWN EXACT SOLUTIONS

Note the earlier result of $\delta(x) \sim c_1\sqrt{x}$ and $f \sim 1/\sqrt{x}$ at $x \sim 0$ is in qualitative agreement with the exact similarity solution (Cess [12], Koh [13], etc.) for laminar (vapor and condensate) film condensation flows over a horizontal ($Fr^{-1} = 0$) plate. The classical solution (Koh [13]) gives

$$\Delta(\chi) \equiv \eta_\delta\sqrt{\mu_1\chi/\rho_1 U} \quad \text{and} \quad \omega_2(\chi, y) \equiv Uf_2'(\xi) \tag{19}$$

where the number η_δ and the function $f_2'(\xi)$ with $\xi \equiv c(y\text{-}\Delta(\chi))/\Delta(\chi)$, $c \equiv \eta_\delta\sqrt{\rho_2\mu_1/\rho_1\mu_2}$ are obtained by a well defined procedure given in Koh [13].

For laminar vapor flow in Fig. 1, in the limit of $h \to \infty$ (i.e. $Re_{in} \to \infty$), it is easy to verify that the classical solution in equation (19) and the interface condition $\tau^i = \mu_2(\partial u_2/\partial y)^i$ would be in quantitative agreement with $\delta(x) = c_1x^{1/2} + \ldots$, in equation (13) and f in equation (12) if and only if $\lim_{Re_{in}\to\infty} c_1\sqrt{Re_{in}}$ and $\lim_{Re_{in}\to\infty} f\sqrt{xRe_{in}}$ exist and satisfy

$$\sqrt{\rho_1\mu_2/\rho_2\mu_1}\lim_{Re_{in}\to\infty}(c_1\sqrt{Re_{in}})=\eta_\delta$$

$$(1/2)\lim_{Re_{in}\to\infty} f\sqrt{xRe_{in}}=f_2''(0). \tag{20}$$

Now c_1 depends on the choice of $u_2(x,y)$. Therefore, if we chose a correct $u_2(x,y)$ profile in our solution method and we are able to numerically verify the equality in equation (20), then it would establish the correctness of the asymptotic friction factor formula and the complex computer based algorithm for finding the root c_1 and other constants. This requires more than merely letting $h\to\infty$ in the analysis for flow between horizontal parallel plates. In the absence of a two-dimensional scheme, to verify equation (20) with the help of the above one-dimensional scheme, we set $Fr^{-1}=0$ and choose the exact velocity profile

$$u_2(x,y)=f_2'(\xi), \tag{21}$$

where $f_2'(\xi)$ is the similarity solution in equation (19) as obtained by the method given in Koh [13]. Furthermore, in one-dimensional formulation, information at $y=1$ (i.e. $y=h$) influences the solution at $y=\delta(x)$ because of the single element (such as ABDC) involved in Fig. 1. Therefore, to simulate actual $u_2(x,y)$ effects, we allow mass flow (using non-zero $v_2(x,1)$ from the similarity solution) out of the plate at $y=h$. This models deflection of streamlines away from the plate as found in the solution (Koh [13]) for flow over the horizontal plate. For large y, assuming velocity and pressure approach the flat plate solution, we set $f_u=0$ (because $u_2(x,y)\approx U$) and require the constants f_{00}, f_{01}, etc. in the interfacial shear expression $f(x)=\bar{f}x^{-1/2}+f_{00}+f_{01}x^{1/2}+,\ \ldots,$ to be such that $d\pi/dx\approx 0$. Here $\bar{f}\equiv 4(c_1+c_2)/Re_1c_1^2$ is obtained by the existence requirement (as in Section 5) and f_{00}, f_{01}, etc. are chosen such that k_1, k_2, etc. are zero (since $d\pi/dx\approx 0$). In accord with the above recommendations, we modify the governing equations (11) and implement the procedure given in Section 5 of Narain [25]. For brevity, we do not give here the modified forms of the resulting equations. Under the above modifications, the one-dimensional approach coincides with a two-dimensional numerical scheme. Representative results in Table 1 numerically verify the equalities in equation (20). Considering the complex, numerous, but very different kinds of steps involved in obtaining η_δ (see Koh [13]) and c_1, the excellent verification of equation (20) in Table 1 is a remarkable validation of the proposed asymptotic form of interfacial shear and the general purpose computational/analytical procedure given here to resolve the elliptic singularity at $x\sim 0$. In Table 1, $h\to\infty$ situation is quickly realized at moderate Re_{in} because gap h quickly becomes larger than vapor boundary layer thicknesses at $x\sim 0$.

7. ASSESSMENT OF POPULAR INTERFACIAL SHEAR MODELS

Once the asymptotic model f_{asy}, the leading term on the right side of equation (12), has been obtained for $0<x<\varepsilon$ for some small ε, one can connect any popular interfacial shear model f_{model} (valid for $x\geqslant\varepsilon$) to f_{asy} by a suitable approach. One connection of f_{asy} to f_{model} is given in equation (20) of Narain [25]. Another connection recommended by us makes use of the observation (see Fig. 5) that f_{asy} typically falls rapidly from large values to small values and, therefore, we can also use:

$$f=f_{model}\left[\frac{\phi}{\exp(\phi)-1}\right]\approx\begin{cases}f_{asy} & \text{for } \phi<-3\\ f_{model} & \text{for } -0.4\leqslant\phi\leqslant 0,\end{cases} \tag{22}$$

where $\phi\equiv -f_{asy}/f_{model}$. The above formula in equation (22) is an adaptation of a recommendation given in Hewitt *et al.* (see p. 603 of Ref. [34]).

At large x, typically less than $O(h)$, it is found that the numerical solution of equation (11) does not depend on a particular method of connecting f_{model} to f_{asy} at $x\sim 0$. Despite the limited practical significance of the question as to what is the right connection of f_{asy} to a good f_{model}, a good scientific answer to this question will have to wait until a sound theoretical understanding (scopes, limitations, range of applicability, etc), is available for a good f_{model}. If the good models sought here are refined and made valid over smooth, nearly smooth, and wavy interface zones; then the issue of connecting f_{asy} to f_{model} would not be significant—except for very tiny distances.

Various choices of f_{model}

There are several recommendations for f_{model} in the literature. We consider here Shekriladze and Gomelauri [26] model, Mickley [33] model or Film theory (see p. 599 of Ref. [34]), Henstock and Hanratty [35] type model for vertical downflow as modified by Andreussi [36], Andreussi model [36] with Shekriladze and Gomelauri [26] type suction effect, single phase flow friction models, generalized Narain [25] type model, and a modified Henstock and Hanratty/Andreussi model. These models are defined in equations (A3)–(A11) of the Appendix. The above representative works have already taken into account several other models which do not work, therefore, there are many other models whose assessments are not reported here. These omitted models can be verified to be ineffective in reasonably predicting annular film condensation flows considered here. Among these are Wallis model (see Carey [41]), etc. In equation (22), we substitute for f_{model} any of the formulas for $f_{model\,i}$ in equations (A3)–A11) and find a corresponding numerical solution of the governing equation (11). In the approach of this paper, all the local flow variables (u_{av}, δ, etc.) used in evaluating these models are such that they exactly satisfy the mass transfer (suction into the film) condition at the interface and, therefore, suction effects are fully accounted for. The models are, therefore, being tested for their hydrodynamic efficacy in modeling interfacial shear.

To test the models, we specify flow parameters to simulate specific experimental situations and then compare theoretically predicted and experimentally obtained values of local ($\hbar_\chi$) or average ($\bar{\hbar}_\chi$) heat transfer coefficients defined in equation (38) of Narain [25]. Note that, even after the resolution of the singularity at $x \sim 0$ by the method given in Section 5, the vector differential equation (11) is stiff and requires fifth- or sixth-order accuracy schemes to be implemented on a sufficiently fast machine in double precision mode.

Relevant experimental data

There are many experimental measurements of average heat transfer co-efficient for specified lengths of internal condensing flows. Here we consider a few representative runs (see Table 2) corresponding to annular negligible entrainment flows and laminar condensates ($Re_L(x) < 1600$) from the following experiments: (i) experiment I (Cavallini and Zecchin [19]) dealing with downflow condensation of R11 vapor in a vertical pipe; (ii) experiment II (Goodykoontz and Dorsch [18]) dealing with condensation of steam in a vertical pipe of non-constant wall temperature $\mathscr{T}_w(\chi)$; and (iii) experiment III (Lu [28]) dealing with condensation of R113 in a horizontal duct of rectangular cross-section. Of the above, experiment III has been observed through transparent walls and is known to belong to the annular zero entrainment flow regime. However, only those representative runs (see Table 2) of experiments I and II are considered here which have been inferred (based on experimental/computational trends and flow regime maps) to belong to the annular negligible entrainment flow regimes. The data from vertical pipe experiments I and II are directly compared with predictions for vertical pipes.

Interestingly, under certain conditions, we can also compare vertical channel predictions with a corresponding vertical pipe (diameter D) experiment provided we set

$$h = D/4, \tag{23}$$

for the characteristic length L_c for channel flows. Now, for equal lengths of the two ducts, equation (23) insures that the ratio A_c/A_{cond} of cross-sectional area A_c to the condensing surface area A_{cond} is the same. If, for the two situations, we also assume that inlet speed U, temperature difference $\Delta\mathscr{T}$, wall temperature $\mathscr{T}_w$, and inlet pressure p_o are the same, then it is reasonable to expect approximate equality of average heat transfer co-efficient $\bar{\hbar}_\chi$. This is because, if the characteristic length given in equation (23) is also used for non-dimensionalizing the flow variables in the vertical pipe situation, then the non-dimensional parameters listed in (2) become identical for the two situations. As a result, the arguments of the liquid fraction z in equation (A13) of the Appendix become the same and, hence, z is the same for the two situations. Therefore, the overall energy balance equation (A13) implies

$$\bar{\hbar}_\chi|_{\text{vertical pipe}} \approx \bar{\hbar}_\chi|_{\text{vertical channel}} \tag{24}$$

Table 2. Shear dominated annular flow experimental runs and theoretical predictions

Experiment	Expt. run no.	U (m/s)	P_o (kPa)	Experimental variable used	Theoretical predictions of the experimental $\hbar_\chi$ or $\bar{\hbar}_\chi$ with $f_{\text{model}\,i}$ (i = 1 to 6) used in equation (22)
No. I. Fluid: R-11 Vertical Cylinder D = 4h = 0.02 m L = 1.7 m $\mathscr{T}_w \cong$ const	34 46 72 74 99	26.85 26.01 11.66 12.25 21.28	111.90 129.80 125.78 125.33 123.09	Value of $\bar{\hbar}_\chi$ at χ = 1.7 m	Agreement within ±25% for i = 5 & 6. No agreement within ±25% for i = 1 to 4.
No. II Fluid: steam Vertical Cylinder D = 4h = 0.016 m L = 2.134 m $\mathscr{T}_w(\chi) \neq$ const. obtained from expt. data.	1 6 5 7	70.71 22.02 20.84 36.22	110.62 310.70 270.13 266.15	Value of $\hbar_\chi$ at χ = 0.51, 1.51, 2.51, 3.51, 4.51 and 5.51 ft	Agreement within ±25% for i = 1 to 6.
No. III Fluid: R-113 Horizontal channel h = 0.025 m, w = 0.04 m L = 1.5 m $\mathscr{T}_w \cong$ const	221 181 248 262 294 288 269 268	0.31 0.50 2.15 2.69 4.06 4.34 1.15 1.40	108.82 111.53 102.39 100.92 102.50 101.49 103.25 99.75	Values of $\hbar_\chi$ at χ = 0.5993 m, and χ = 0.8990 m	Agreement within ±25% for i = 5 & 6. No agreement within ±25% for i = 1 to 4.

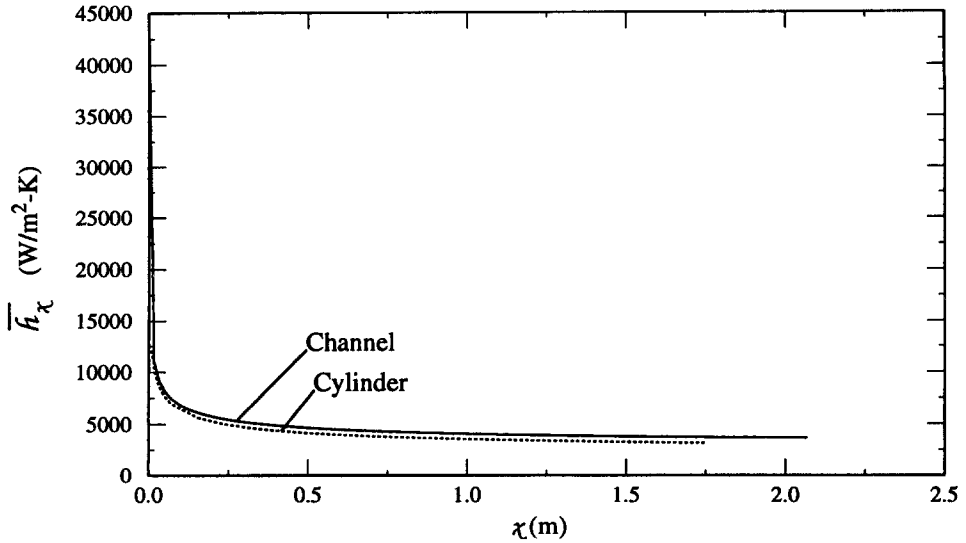

Fig. 2. The above figure compares the average heat transfer coefficient $\bar{h}_\chi$ for a specific representative flow situation given by run no. 46 of Experiment I in Table 2. The computation employs $f_{\text{model 6}}$ given in (A11).

for any length χ within the annular regime under consideration. As we see in Fig. 2, the more detailed solution of equation (11) for the two flows is in agreement with equation (24). The fluid properties (using ASHRAE Handbook [45]) for the experimental runs considered here restrict us to the parameter range in equation (A14) for channel flows and the parameter range in equation (A15) for downflow in pipes.

Assessments

The results for vertical or horizontal channel situations are shown in Table 2 and this indicates that none of the popular models uniformly do well for all the three experiments in Table 2. For example, the models $f_{\text{model 1}}$ through $f_{\text{model 4}}$ in equations (A3)–(A9) of the Appendix are adequate for steam in expt. II but they are inadequate for R11 in expt. I or R113 in expt. III. However, the modified Andreussi model $f_{\text{model 6}}$ in equation (A11) and Narain [25] type $f_{\text{model 5}}$ in equation (A10) do well for experiments I, II and III. The results for downflow in vertical pipes, because of (24), remain much the same.

Note that the vertical situations (experiments I and II) will differ from the horizontal situation (experiment III) in the wavy structure of the interface. Therefore, we do not expect that a model for the vertical configuration would, in general, work for the horizontal configuration. However, what is clearly inadequate is that the existing models $f_{\text{model 1}}$ through $f_{\text{model 4}}$ in equations (A3)–(A9) do not uniformly work for both experiments I and II.

Identification/proposal of some adequate or good models

The detailed predictions (not shown here) of Andreussi Model [36] $f_{\text{model 4}}$ is reasonable (nearly within $\pm 25\%$) for experiment I and qualitatively correct for experiment II. The lack of quantitative agreement is due perhaps to the density ratio ρ_2/ρ_1 being significantly out of range of the original Henstock and Hanratty [35] considerations. For turbulent flows, density ρ_2 is very important in affecting near interface turbulence and drag. Hence, the proposed replacement of the function $\hat{f}(\rho_2/\rho_1)$ in equation (A8) by $\hat{f}_{\text{modified}}(\rho_2/\rho_1)$ in equation (A11) produces reasonable results for experiment I, experiment II and in a sense to be described, smooth interface regime of experiment III as well. Therefore, $f_{\text{model 6}}$ seems promising and appears to be a good candidate for further development.

The Narain [25] type model is known to be adequate for the horizontal channel flow. Its obvious generalization in equation (A10) of the Appendix is also promising and can be developed (i.e. correlation for β can be obtained) if sufficient experimental data is available in a suitable form.

Regularities in our calculations and assessments

- For a chosen f_{model}, say modified Andreussi model in equation (A11), we solve for flows in a vertical channel and a vertical pipe under similar conditions and by incorporating the required asymptotic behavior of f through equation (22). The approximate equality expected in equation (24) implies approximate equality of the local heat transfer coefficient h_χ. Representative calculations shown in Fig. 2 meet this expectation and support the correctness of our calculations and calculation procedure.
- Andreussi model [36] in equation (A6)–(A8) is supposed to work for downward vertical gas/liquid annular flows (from *ripples* zone to larger amplitude *disturbance wave* regime under negligible entrainment conditions). Therefore, we find, the modified Andreussi model in equation (A11) for f_{model} in equation (22), works well for the vertical condensing

flows considered here. However, for estimating the interfacial shear, and for help in separating the effects of relative speed (u_{av}-u_f) of vapor with respect to the interface from the effects of the structure of waves on the interface, it is good (see Hewitt and Govan [46]) to use relative friction factor f_{rel} in equation (3). Therefore, if we define

$$\tau^i_{vert} \equiv \frac{1}{2}\rho_2(Uu_{av}(x))^2 f_{vert} = \frac{1}{2}\rho_2 U^2(u_{av}-u_f)^2 f_{vert\,rel} \tag{25}$$

the relative speed based friction factor $f_{vert\,rel}$ for the vertical configuration can be numerically obtained through the above equation (25) as f_{vert} and u_f are known through our one dimensional computational solution of equation (11). This is necessary because direct use of relative friction factor is not recommended here. This is because u_f, evaluated as $u_1(x, \delta(x))$ in equation (5), would become unnecessarily complex if f_{rel} (instead of f) is used and this would also lead to a far more complex formulation than equation (11).

We expect, particularly for smooth (or nearly smooth ripple interface) vertical channel flows, that $f_{vert\,rel}$ should be nearly equal (or nearly equal) to the relative speed based friction factor $f_{horiz\,rel}$ if the corresponding channel flow in the horizontal configuration is also a smooth interface flow. This is because differences in the physical values of τ^i for such situations are largely due to differences in the relative speed (u_{av}-u_f). For brevity, without showing the calculations, we merely assert that our calculations support the expectation that $f_{horiz\,rel}(x) \approx f_{vert\,rel}(x)$ if the two flows are nearly smooth. However, as expected, this is not true for significantly wavy flows because the two wavy structures are very different.

8. ASSESSMENT OF HEAT TRANSFER CORRELATIONS

There are several heat transfer correlations available for internal condensing flows in vertical pipes. These are typically given in terms of internal flow variables (such as local values of condensate Reynolds number, the ratio of cross-sectional vapor mass flow to total mass flow rate, etc.) and cannot be assessed without a reliable predictive tool or direct and independent experimental measurements of the internal variables. Therefore, we solve equation (11) for cylindrical geometry, with f as in equation (22) and f_{model} given by $f_{model\,6}$ in equation (A11) of the Appendix. The theoretical predictions are used to calculate average heat transfer co-efficients and these predictions are then also compared with the values obtained by theoretically evaluating some well known correlations for local heat transfer coefficients. Here we consider: (i) correlation 1 which is Traviss *et al.* [39] correlation given in Carey [41]; (ii) correlation 2 which is Shah [20] correlation given in Carey [41]; and (iii) correlation 3 which is the correlation given in Numrich [40]. The results, not shown here for brevity, indicates that correlation 1 is good to satisfactory (nearly within $\pm 25\%$) for experiment I and poor (not within $\pm 30\%$) for experiment II, correlation 2 is satisfactory (within $\pm 35\%$) for experiments I and II, and correlation 3 is good (within $\pm 10\%$) for experiment I and poor (not within $\pm 30\%$) for experiment II.

Although the Shah [20] correlation is satisfactory for the parameter range considered here, the above assessments demonstrate the need for better defined and more reliable heat transfer correlations. Furthermore, we have shown that development of more accurate and well defined interfacial shear models would automatically lead to better predictions of heat transfer coefficients. These predicted values can then be correlated for direct use.

9. OPEN ISSUES

This paper outlined an approach for the development of theoretical/computational predictive abilities. However, it also establishes the need for addressing the following issues:

- More general experimental development of flow regime maps for specific flow geometries covering a suitable range of the parameters in (2), a surface tension parameter (say $\sigma\rho_1 L_c/\mu_1^2$), and a parameter representing the normal component of gravity (say $g_y L_c/U^2$). Such maps can, in particular, more reliably identify negligible entrainment annular flow regimes.
- More accurate experimental measurements of mean film thickness, mean pressure drops, etc. in addition to measurements of local or average heat transfer coefficients. This would allow development of more effective and reliable interfacial shear models. If suitable experiments covering commonly occurring range of parameter values in (2) become available, the approach of this paper can yield good interfacial shear models and detailed analytical/computational predictive abilities.
- More accurate experimental measurements of local flow variables in real time are needed for assistance in: (i) developing a criteria better than $Re_L(x) < 1600$ to mark liquid condensate's transition from laminar to turbulent regime; (ii) developing a good rule for determining when the vapor core is laminar or turbulent (this should be done in the light of relaminarization expected for turbulent vapor flows as they slow down in the downstream regions); and (iii) developing a qualitative characterisation of interfacial wave structures and their relationship to models for mean interfacial shear.

10. DISCUSSIONS AND RESULTS

The asymptotic form of friction factor model given in equation (9) is derived from a simple physical argu-

ment and is the general form of a related result given in Narain [25]. This asymptotic form of friction factor is satisfied by the classical exact solutions of Sparrow and Gregg [3], Koh [13], etc. and is shown here to be the required solvability condition for analytical/computational solution of flows in tilted channels and vertical pipes. Therefore, at the point of onset of condensation, this asymptotic form should be used in place of the asymptotic models of Shekriladze and Gomelauri [26] or other related models (Jensen and Yuen [47], Linehan *et al.* [48], etc.). The idea behind the model of Shekriladze and Gomelauri [26] type models is simple and slightly flawed for internal flow situations. This model recognizes the importance of mass transfer and associated momentum transfer across the interface and attempts to put this effect in the form of an "effective" interfacial shear. The first flaw comes from the assumption that it is the momentum flux contribution $\dot{m}Uu_{av}$ (see equation (A3)) representing the momentum upstream of $x = 0$ (assuming uniform flow at inlet) which is relevant for determining interfacial shear, whereas, in fact, it is the contribution $\dot{m}u_1^i (= \dot{m}Uu_f)$ from the near interface locations that are quantitatively more relevant. In this sense, Shekriladze and Gomelauri [26] and related models merely assert that we drop the interface momentum transfer term called the "kick back" term (i.e. the third term on the left side of the vapor momentum balance equation (9) of Narain [25]) and build its effect into a suitable expression for an interfacial shear model f. A substitution of equation (A3), after replacing $\dot{m}Uu_{av}$ by $\dot{m}Uu_f$, for f in equation (9) of Narain [25], while dropping the "kick back" term, confirms that this indeed is the essential idea. The second flaw in this model comes from the basic result of this paper that, even after correctly accounting for momentum transfer, the asymptotic form of shear is not determined by this phenomenon at $x \sim 0$. In fact, a combined consideration of all the governing equations in equation (11) has established that the dominant effect on the asymptotic form of interfacial shear is controlled by mass balance while the interfacial momentum transfer plays a lesser role for internal flow situations.

Despite the clear evidence above of inadequacy of Shekriladze and Gomelauri [26] and related asymptotic shear models for internal flows, we would like to assert that we have not investigated this model's capability for external condensing flows over cylinders. In fact a significant amount of work in this area (Rose [49], Michael *et al.* [50], Memory and Rose [51], etc.) report that Shekriladze and Gomelauri [26] model is good for studying condensate thickness variations in this external flow situation. Perhaps this is due to the external nature of the near interface vapor boundary layer in these studies and perhaps this is also due to the fact that there are no locations where film thickness Δ is zero.

Using a computer algebra based analytical/computational non-linear analysis, we showed (Section 5) how to use the above solvability condition towards resolving the "elliptic" singularity at the point of onset of condensation ($x = 0$). This method probes the nature of solution at short downstream locations until convergence (at $x \sim 0$) is achieved. In Sections 4–6 we showed that the above resolution of singularity can lead to effective one- (or two-) dimensional numerical solution schemes. The one-dimensional scheme is implemented here and the results of the two-dimensional scheme will be reported in future works. The novel algorithm of resolving the singularity is shown, in Section 6, to yield results in excellent agreement with the exact similarity solutions (Koh [13], etc.) for film condensation.

The assessments of various interfacial shear models in Table 2 indicates that, except for Model 5 and Model 6, there are no reliable and reasonably accurate models currently available for internal "annular" film condensation situation. Our identification/proposal is that modified Andreussi model (Model 6 in equation (A11)) for vertical configuration and Narain type model (Model 5 in equation (A10)) for all configurations show promise and should be developed with the help of further experiments and theoretical/computational predictions.

The assessment of some representative heat transfer correlations show the adequate nature of Shah [20] correlation for the flows considered here. We know from Narain [25] that the one dimensional scheme properly predicts the average vapor speed $u_{av}(x)$ and the mean film thickness $\delta(x)$ quite reliably for a "good" friction factor model. There it was shown that the one-dimensional solution for u_{av} and δ, away from $x \sim 0$, is insensitive to the actual cross-sectional variations in vapor velocity and to the vapor entry conditions (whether fully developed or uniform). The variables $u_{av}(x)$ and $\delta(x)$ control the motion of the liquid condensate and are somewhat insensitive to modest changes (see Narain [25]) in pressure $\pi(x)$ for different vapor entry conditions. Since the average pressure variations $\pi(x)$ are affected (see Narain [25]) by entrance conditions, a two-dimensional numerical solution scheme is needed for this variable.

In Fig. 3 we show how the liquid condensate thickens when a tilted channel ($Fr^{-1} = 0.053$) is made horizontal ($Fr^{-1} = 0$). The downstream thinning of the condensate in the vertical situation of Fig. 3 is due to the gravitational acceleration of the condensate. Equations (17)–(18) assert that this thinning does not happen for the shear dominated portion at $x \sim 0$; in fact there is a thickening of the condensate here. This is because, at $x \sim 0$, gravity is able to reduce interfacial shear without being able to significantly accelerate the liquid condensate (velocity is very nearly given by equation (6)). Although not shown here for brevity, as expected, the faster condensate drainage in the vertical situation causes much lower $u_{av}(x)$ values as compared to the corresponding horizontal situation. For predictions in Figs. 3–5, we used the "good" Modified Henstock and Hanratty/Andreussi model (equation

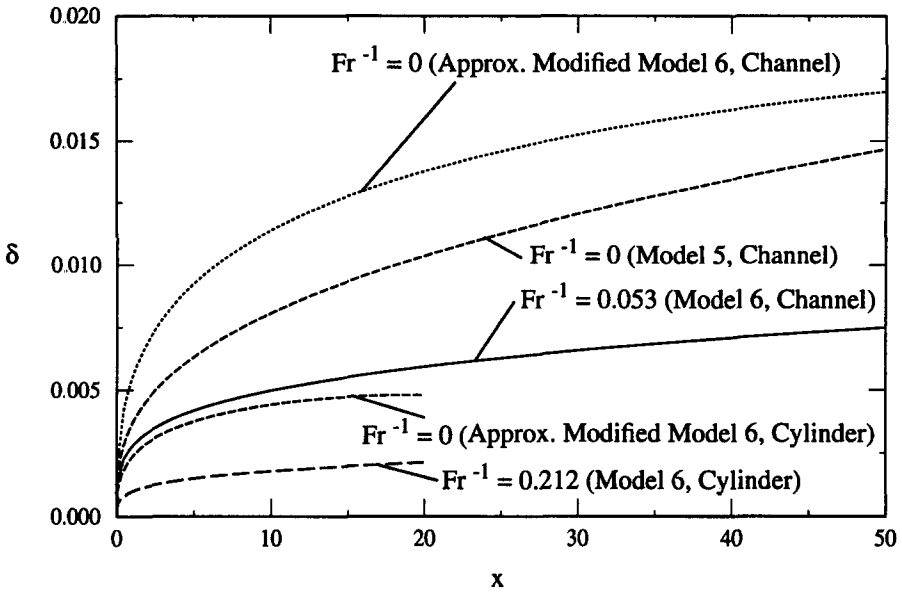

Fig. 3. The horizontal flow situation ($Fr^{-1} = 0$) above is specified by run no. 248 of Experiment III in Table 2. The predictions for the horizontal configuration are done by the "good" Model 5 ($\beta = 4.1$, see Narain [25]) and the approximate Model 6 (by setting $f_{rel}|_{Fr^{-1}\neq 0} \approx f_{rel}|_{Fr^{-1}=0}$). The predictions for the vertical configuration ($Fr^{-1} = 0.053$) are for the same flow except for the change in orientation. The predictions for downflow in cylinders, with gravity ($Fr^{-1} = 0.212$) or without gravity ($Fr^{-1} = 0$), are for the same flow with $x \equiv \chi/L_c$ and $L_c = D = 4h$.

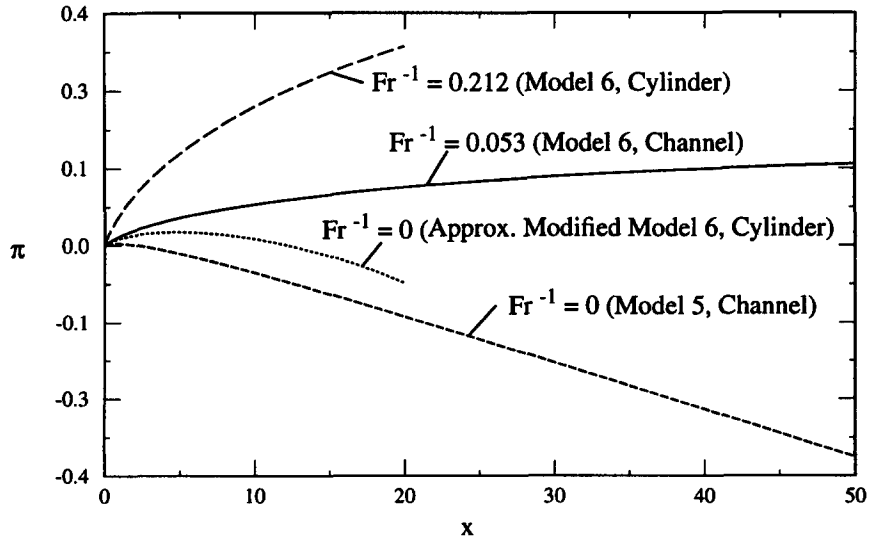

Fig. 4. For each flow situation described in Fig. 3 for predicting film thickness δ, the corresponding predictions of the non-dimensional pressure π are shown above.

(A11)) in equation (22) for the $Fr^{-1} \neq 0$ situation and an approximate model, obtained by setting $f_{rel}|_{Fr^{-1}\neq 0} \approx f_{rel}|_{Fr^{-1}=0}$, for the $Fr^{-1} = 0$ situation. Note that a better prediction for the horizontal configuration ($Fr^{-1} = 0$) is obtained for channel flows by employing Model 5 of Narain [25], the results for this model are also shown in Figs 3 and 4. The pipe flow and channel flow situations are the same except, for pipe flow, $x \equiv \chi/L_c$ and $L_c = D = 4h$. As expected, in Fig. 4, we see that the gravitational assistance in condensate removal leads to much smaller needs in pressure drop (or pumping power). In fact for vertical ($Fr^{-1} = 0.053$) channel flow configuration, at many locations in Fig. 4, there is a pressure recovery ($\pi > 0$) and this is feasible (e.g. see some pressure drop data in Fig. 6 of Owen *et al.* [52]) and interesting. Increasing average $\pi(x)$ or pressure recovery for this gravity assisted ($Fr^{-1} = 0.053$) situation is consistent with the deceleration of the vapor flow needed to sufficiently reduce vapor speeds so as to meet the demands of increased condensation rate associated with thinner condensate and faster drainage. The pressure results

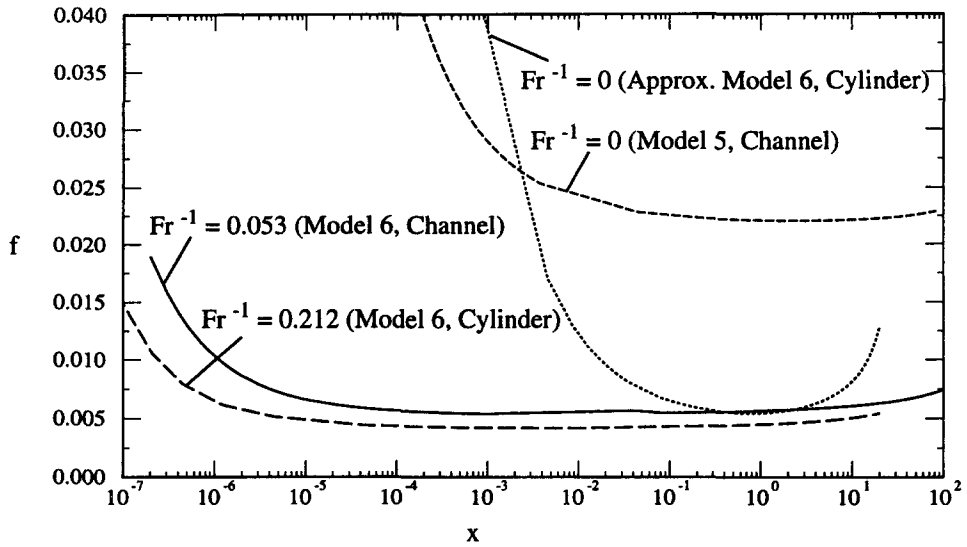

Fig. 5. The predictions of the friction factor f are for R113 vapor flow conditions specified by run no. 248 of experiment III in Table 2. The horizontal channel has $Fr^{-1} = 0$ and the vertical channel has $Fr^{-1} = 0.053$. The $Fr^{-1} = 0$ horizontal channel situation employs the "good" $f_{\text{model 5}} = \beta f_{\text{o}}$, $\beta = 4.1$ in equation (22). The values for $Fr^{-1} = 0$ case for cylinders is obtained by using $f_{\text{model 6}}$ for the vertical ($Fr^{-1} = 0.212$) configuration and then modifying these values under the assumption $f_{\text{rel}}|_{Fr^{-1}\neq 0} \approx f_{\text{rel}}|_{Fr^{-1}=0}$.

for downflow in a vertical pipe in terrestrial environments ($Fr^{-1} = 0.212$) and in micro-gravity environments ($Fr^{-1} = 0$) were obtained along with the film thickness results in Fig. 3. For the flow situation considered in Figs 3 and 4, some of the actual variations in the interfacial friction factor f are shown in Fig. 5. Note that physical values of interfacial shear τ^{i}, given by equation (3), are quite different for the vertical and the horizontal situations because of significant differences in the values of average vapor speed $u_{\text{av}}(x)$. The trends of the variables δ, u_{av} and π with changes in speed U (or Re_{in}) and temperature difference $\Delta\mathcal{T}$ (or Ja/Pr_{l}) are similar to those for the horizontal situation given in Narain [25] and Narain [42].

11. CONCLUSIONS

- We presented a new and general asymptotic form of interfacial shear (for large condensation rates at the onset of condensation) required for the solution of the classical equations modeling annular film condensation.
- We demonstrated that traditional asymptotic interfacial shear models do not work for internal annular flows.
- We presented a novel computer algebra based analytical/computational nonlinear analysis and algorithm for resolving the singularity at $x \sim 0$. We also showed that this algorithm yields results in agreement with well-known exact solutions of film condensation.
- We implemented a one-dimensional computational scheme for downflow in channels and vertical pipes. We showed the value of this approach for forthcoming two-dimensional computational simulations.
- We assessed popular interfacial shear models for their validity at points away from the singularity and proposed/identified two good models which may need further improvements.
- We showed the value of this approach in evaluating and proposing heat transfer correlations.
- We showed that our computations have many regularities for problems with constant or variable condensing surface temperatures.

REFERENCES

1. Nusselt, W., Die Oberfalchenkondesation der Wasserdampfes. *Zeitschrift des Vereines Deutschen Ingenieure*, 1916, **60,** 541–546.
2. Rohsenow, W. M., Heat transfer and temperature distribution in laminar film condensation. *ASME Transactions*, 1956, **78,** 1645–1648.
3. Sparrow, E. M. and Gregg, J. L., A boundary layer treatment of laminar film condensation. *ASME Journal of Heat Transfer*, 1959, **81,** 13–18.
4. Koh, J. C. Y., Sparrow, E. M. and Hartnett, J. P., The two-phase boundary layer in laminar film condensation. *International Journal of Heat and Mass Transfer*, 1961, **2,** 69–82.
5. Chen, M. M., An analytical study of laminar film condensation: part 1—flat plate. *Journal of Heat Transfer*, 1961, **83,** 48–54.
6. Dhir, V. K. and Lienhard, J. H., Laminar film condensation on plane and axisymmetric bodies in nonuniform gravity. *J. Heat Transfer*, **93,** 97–100 (1971).
7. Sadasivan, P. and Lienhard, J. H., Sensible heat correction in laminar film boiling and condensation. *Journal of Heat Transfer*, 1987, **109,** 545–546.
8. Kutateladze, S. S., *Fundamental of Heat Transfer*, Academic Press, New York, 1963.
9. Labuntsov, D. A., Heat transfer in film condensation of

pure steam on vertical surfaces and horizontal tubes. *Teplaenergentica*, 1957, **4,** 72. Also see Heat transfer during condensation of steam on a vertical surface in conditions of turbulent flow of a condensate film, *Inghenerno-Fizicheski Zhurnal*, 1960, **3,** 3–12 (in Russian).
10. Gregorig, R., Ken, J. and Turek, K., Improved correlation of film condensation data based on a more rigorous application of similarity parameters. *Wärme-und Stoffübertragung*, 1974, **7,** 1–30.
11. Fujii, T. and Uehara, H., Laminar filmwise condensation on a vertical surface. *International Journal of Heat and Mass Transfer*, 1972, **15,** 217–233.
12. Cess, R. D., Laminar film condensation on a flat plate in the absence of a body force. *Zeitschrift für Angewandte Mathematik und Physik*, 1960, **11,** 426–433.
13. Koh, J. C. Y., Film condensation in a forced-convection boundary-layer flow. *International Journal of Heat and Mass Transfer*, 1962, **5,** 941–954.
14. Shekriladze, I. G. and Mestvirishvilli, S. A., Study of the process of film condensation of a flowing vapor within a vertical tube. *Heat Transfer—Soviet Research*, 1972, **4,** 1–6.
15. Dobran, F. and Thorsen, R. S., Forced flow laminar filmwise condensation of a pure saturated vapor in a vertical tube. *International Journal of Heat and Mass Transfer*, 1980, **23,** 161–177.
16. Wang, C. Y. and Tu, C. J., Effects of non-condensable gas on laminar film condensation in a vertical tube. *International Journal of Heat and Mass Transfer*, 1988, **31,** 2339–2345.
17. Carpenter, F. G. and Colburn, A. P., The effect of vapor velocity on condensation inside tubes. *Proceedings of the General Discussion of Heat Transfer*, The Institute of Mechanical Engineers and the ASME, July 1951, pp. 20–26.
18. Goodykoontz, J. H. and Dorsch, R. G., Local heat-transfer co-efficients for condensation of steam in vertical downflow within a 5/8-inch-diameter tube. NASA TND-3326, March '66, 1966, pp. 1–44.
19. Cavallini, A. and Zecchin, R., High velocity condensation of R-11 vapors inside vertical tubes. *Heat Transfer in Refrigeration*, International Institute of Refrigeration, 1971, pp. 385–396.
20. Shah, M. M., A general correlation for heat transfer during film condensation inside pipes. *International Journal of Heat and Mass Transfer*, 1979, **22,** 547–556.
21. Dukler, A. E., Characterization, effects and modeling of the wavy gas–liquid interface. *Progress in Heat and Mass Transfer*, 1972, **6,** 207–234.
22. Dukler, A. E., The role of waves in two-phase flow: some new understanding. *Chemical Engineering Education*, 1976 Award Lecture, 1977, pp. 108–138.
23. Hanratty, T. J., Interfacial instabilities caused by air flow. In *Waves on Fluid Interfaces*, Ed. R. E. Meyer. Academic Press, New York, 1983.
24. Moody, L. F., Friction factors for pipe flow. *ASME Transactions*, 1944, **66,** 671–684.
25. Narain, A., Modeling of interfacial shear and heat transfer predictions for internal flows with film condensation. *Journal of Applied Mechanics*, 1996, **63,** 529–538.
26. Shekriladze, I. G. and Gomelauri, V. I., Theoretical study of laminar film condensation of flowing vapor. *International Journal of Heat and Mass Transfer*, 1966, **9,** 581–591.
27. Chen, S. L., Gerner, F. M. and Tien, C. L., General film condensation correlations. *Experimetal Heat Transfer*, 1987, **1,** 93–107.
28. Lu, Q., An experimental study of condensing heat transfer with film condensation in a horizontal rectangular duct. Ph.D. thesis, Michigan Technological University, Houghton, Michigan, 1992.
29. Lu, Q. and Suryanarayana, N. V., Condensation of a vapor flowing inside a horizontal rectangular duct. *Journal of Heat Transfer*, 1995, **117,** 418–424.
30. Bell, K. J., Taborek, J. and Fenoglio, F., Interpretation of horizontal in-tube condensation heat transfer correlations with a two-phase flow regime map. *Chemical Engineering Progress Symposium Series*, 1970, **66,** 150–163.
31. Palen, J. W., Breber, G. and Taborek, J., Predictions of flow regimes in horizontal tube condensation, *Heat Transfer Engineering*, 1979, **1,** 47–57.
32. Soliman, M., Schuster, J. R. and Berenson, P. J., A general heat transfer correlation for annular flow condensation. *Journal of Heat Transfer*, 1986, **90,** 267–276.
33. Mickley, H. S., Heat, mass and momentum transfer for flow over a flat plate with blowing or suction. NASA Report, NACA-TN-3208, 1954.
34. Hewitt, G. F., Shires, G. L. and Bott, T. R., *Process Heat Transfer*. CRC Press, FL, 1994.
35. Henstock, W. H. and Hanratty, T. J., The interfacial drag and height of the wall layer in annular flows. *American Institute of Chemical Engineers Journal*, 1976, **22,** 990–1000.
36. Andreussi, P., The onset of droplet entrainment in annular downward flows. *The Canadian Journal of Chemical Engineering*, 1980, **58,** 267–270.
37. Spedding, P. L. and Hand, N. P., Prediction of holdup and pressure loss from the two phase momentum balance for stratified type flows. In *Advances in Gas-Liquid Flows* 1990, edited by J. H. Kim, V. S. Rohtagi and A. Hashemi, ASME FED-Vol. 99 and HTD-Vol. 155, 1990, pp. 73–87.
38. Wallis, G. B., *One-Dimensional Two-Phase Flows*, Wiley, New York, 1965.
39. Traviss, D. P., Rohsenow, W. M. and Baron, A. B., Forced-convection condensation inside tubes: a heat transfer equation for condenser design. *ASHRAE Transactions*, 1973, **79,** 157–165.
40. Numrich, R., Partial condensation in vertical tubes under increased pressures. *Condensation and Condenser Design*, edited by J. Taborek, J. Rose and I. Tanasawa. United Engineering Trustees, ISBN no. 0-7918-0693-6, 1993, pp. 231–246.
41. Carey, V. P., *Liquid–Vapor Phase-Change Phenomena*. Series in Chemical and Mechanical Engineering, Hemisphere, New York, 1992, p. 442.
42. Narain, A., Interfacial shear modeling and flow predictions for internal flows of pure vapor experiencing film condensation. IMA Preprint Series #1103, Institute for Mathematics and Its Applications, University of Minnesota, Minneapolis, 1993.
43. Alekseenko, S. V., Nakoryakov, V. E. and Pokusov, B. G., *Wave Flow of Liquid Films*. Begell House, 1994.
44. Chen, I. Y. and Kocamustafaogullari, G., Condensation heat transfer studies for stratified, co-current two-phase flow in horizontal tubes. *International Journal of Heat and Mass Transfer*, 1987, **30,** 1133–1148.
45. ASHRAE Handbook, Fundamentals SI Edition, American Society of Heating, Refrigeration and Air-Conditioning Engineers, Atlanta, GA, 1985.
46. Hewitt, G. F. and Govan, A. H., Phenomena and prediction in annular two-phase flow. In *Advances in Gas-Liquid Flows* 1990, edited by J. H. Kim, V. S. Rohtagi and A. Hashemi, ASME FED-Vol. 99 and HTD-Vol. 155, 1990, pp. 41–55.
47. Jensen, R. J. and Yuen, M. C., Local heat and mass transfer correlation in horizontal stratified concurrent flow. *Proceedings of the 7th International Heat Transfer Conference*, 1982, pp. 95–100, Munich.
48. Linehan, J. H., Petrick, M. and El-Wakil, M. M., On the interface shear stress in annular film condensation. *ASME Journal of Heat Transfer*, 1969, 450–452.
49. Rose, J. W., Effect of pressure gradient in forced convection film condensation on a horizontal tube. *International Journal of Heat and Mass Transfer*, 1984, **27,** 39–47.

50. Michael, A. G., Marto, P. J., Wanniarachchi, A. S. and Rose, J. W., Effect of vapor velocity during condensation on horizontal smooth and finned tubes. In *Heat Transfer with Phase Change*, edited by I. S. Habib and R. J. Dallman, ASME HTD-Vol. 114, 1989, pp. 1–10.
51. Memory, S. B. and Rose, J. W., Effect of variable viscosity in the pressure of variable wall temperature on condensation on a horizontal tube. *International Journal of Heat and Mass Transfer*, 1994, **37**, 2321–2326.
52. Owen, R. G., Sardesai, R. G. and Butterworth, D., Two phase pressure drop for condensation inside a horizontal tube. In *Heat Exchangers—Theory and Practise*, edited by J. Taborek, G. F. Hewitt and N. Afgan. Hemisphere Publishing Company, New York, 1983, pp. 67–82.

APPENDIX A

The new definitions of A_{22} and b_1 are

$$A_{22} \equiv -\frac{\rho_2}{\rho_1}\left(\frac{1-2\delta(x)}{4}\right)\delta(x), \tag{A1}$$

$$b_1 \equiv -\frac{1}{\delta(4-5\delta)}\left[\frac{1}{Re_1}\frac{3}{\delta^2}\{1-u_{av}(1-2\delta)^2\} - u_{av}^2 f(3-4\delta)\right] + \frac{\rho_1}{\rho_2}Fr^{-1}. \tag{A2}$$

Shekriladze and Gomelauri model [26]

Using the notation in equation (3), this model is given by:

$$\tau^i = \dot{m}[Uu_{av}(x)] \quad \text{or} \quad f_{\text{model 1}} = 2\frac{\rho_1}{\rho_2}\frac{\dot{m}(x)}{u_{av}(x)}. \tag{A3}$$

Mickley [33] *or film model*

Considering single phase channel flow friction f_o for turbulent flows, this model is

$$f_{\text{model 2}} = f_0[\phi_1/(\exp(\phi_1)-1)] \tag{A4}$$

where $\phi_1 \equiv -f_{\text{model 1}}/f_0$, $f_0 \equiv 0.0713\,(Re_2 u_{av}(x))^{-0.25}$ and $f_{\text{model 1}}$ is given in equation (A3).

Andreussi [36] *or Henstock and Hanratty* [35] *Model*:

The definition of this model uses f_0 defined in equation (A4) and the following quantities:

$$\dot{m}'_L \equiv \rho_1\int_0^{\Delta} u_1 \mathrm{d}y, \quad \dot{m}'_G \equiv \rho_2\int_{\Delta}^{h} u_2 \mathrm{d}y$$

$$Re_L \equiv 4\dot{m}'_L/\mu_1 = 4Re_1\int_0^{\delta} u_1 \mathrm{d}y, \quad Re_G = 4\dot{m}'_G/\mu_2$$

$$\tau^* \equiv \tau^i/\rho_1 g_x \Delta. \tag{A5}$$

Using equation (A5), this model is given by

$$f_{\text{model 3}} = f_0[1+1400F\Psi] \tag{A6}$$

where

$$F \equiv \frac{[(0.707Re_L^{0.5})^{2.5}+(0.0379Re_L^{0.9})^{2.5}]^{0.4}}{Re_G^{0.9}}\frac{\mu_1}{\mu_2}\hat{f}\left(\frac{\rho_2}{\rho_1}\right)$$

$$\Psi \equiv \begin{cases} 0.27(\tau^*)^{2/3} & \text{for } \tau^* \leqslant 1.8 \\ 0.33(\tau^*)^{1/3} & \text{for } 1.8 < \tau^* < 30 \end{cases} \tag{A7}$$

and the function $\hat{f}(\rho_2/\rho_1)$ in Andreussi [36] is

$$\hat{f}(\rho_2/\rho_1) = \sqrt{\rho_2/\rho_1}. \tag{A8}$$

Note that Henstock and Hanratty [35] originally recommended $\Psi = \{1-\exp(-\tau^*)\}$ for Ψ in equation (A7).

Andreussi [36] *model with Shekriladze and Gomelauri* [26] *asymptotic behavior*

This model is given by

$$f_{\text{model 4}} = f_{\text{model 3}}[\phi_2/(\exp(\phi_2)-1)], \tag{A9}$$

where $\phi_2 \equiv -f_{\text{model 1}}/f_{\text{model 3}}$.

Narain [25] *model for horizontal channel flows*

This model is given by

$$f_{\text{model 5}} = \beta f_o(x) \tag{A10}$$

where $f_o(x)$ is given in equation (A4) and the number β as a function $\beta\,(Re_{in}, Ja/Pr_1, \mu_2/\mu_1, Fr^{-1}, \rho_2/\rho_1)$ is to be developed. In Table 2, we selected β for each specific flow situation so as to make the predictions agree with experiments. A correlation for β, for $Fr^{-1}=0$, with the remaining parameters in a restricted range, is given in Narain [25].

Modified Henstock and Hanratty/Andreussi model

This model is the same as the Andreussi model [36] in equations (A5)–(A8) except that the function $\hat{f}(\rho_2/\rho_1)$ in equation (A8) has been replaced by $\hat{f}_{\text{modified}}$ given below:

$f_{\text{model 6}} = f_{\text{model 3}}$ except

$$\hat{f}_{\text{modified}}(\rho_2/\rho_1) = \begin{cases} 0.001235\ln(\rho_2/\rho_1)+0.00957 \\ \qquad \text{for } 0.0005 \leqslant \dfrac{\rho_2}{\rho_1} \leqslant 0.00182 \\ 0.05900\ln(\rho_2/\rho_1)+0.37900 \\ \qquad \text{for } 0.00182 \leqslant \dfrac{\rho_2}{\rho_1} \leqslant 0.005 \end{cases} \tag{A11}$$

Overall energy balance

Overall energy balance for a control volume (of cross-sectional area A_c and condensing surface area A_{cond}) bounded by the two plates at $y=0$ and $y=h$, $\chi=0$ and some $\chi>0$ in Fig. 1, is essentially

$$\dot{m}_{total}\mathscr{h}_g^\circ \approx \dot{Q}_{cv} + \dot{m}'_L\mathscr{h}_f^\circ + \dot{m}'_G\mathscr{h}_g^\circ \tag{A12}$$

where $\dot{m}_{total} = \rho_2 U A_c$, $\dot{m}'_L$, $\dot{m}'_G$, $\dot{Q}_{cv}$, $\mathscr{h}_g^\circ$, $\mathscr{h}_f^\circ$ and $\mathscr{h}_{fg}^\circ$ are, respectively, the total mass flux, the cross-sectional liquid mass-flux at χ, the cross-sectional vapor mass flux at χ, the heat removal rate from the condensing surface, enthalpy of saturated vapor at a representative pressure ($\approx p_o$), enthalpy of saturated liquid at a representative pressure ($\approx p_o$), and the heat of vaporization. With $\dot{Q}_{cv} \equiv \bar{h}_x A_{cond}\Delta\mathscr{T}$ and mass balance requirement $\dot{m}_{total} = \dot{m}'_G + \dot{m}'_L$, equation (A12) becomes

$$\bar{h}_x = z(\rho_2 U)(A_c/A_{cond})(1/(\Delta\mathscr{T}))(1/\mathscr{h}_{fg}^\circ) \tag{A13}$$

where $z = \dot{m}'_L/\dot{m}'_G = z(x, Re_{in}, Ja/Pr_1, Fr^{-1}, \rho_2/\rho_1, \mu_2/\mu_1)$.

The arguments of the liquid fraction z at any x follows from the definition of $\dot{m}'_L$ and $\dot{m}'_G$ given in equation (A5) and the non-dimensionalization of variables leading to the list in (2).

Parameter range

Experimental runs considered here restrict us to the following parameter range for channel flows:

$$0.0006 \leqslant \frac{\rho_2}{\rho_1} \leqslant 0.0054,\ 0.016 \leqslant \frac{\mu_2}{\mu_1} \leqslant 0.06,$$

$$0.005 \leqslant \frac{Ja}{Pr_1} \leqslant 0.045$$

$$5660 \leqslant Re_{in} \leqslant 90\,000 \quad \text{and} \quad 0 \leqslant Fr^{-1} \leqslant 0.2 \qquad \text{(A14)}$$

and to the following parameter range for downflow in vertical pipes:

$$0.0006 \leqslant \frac{\rho_2}{\rho_1} \leqslant 0.005,\ 0.018 \leqslant \frac{\mu_2}{\mu_1} \leqslant 0.06,$$

$$0.005 \leqslant \frac{Ja}{Pr_1} \leqslant 0.02$$

$$36\,500 \leqslant Re_{in} \leqslant 340\,000 \quad \text{and} \quad 0 \leqslant Fr^{-1} \leqslant 0.24 \qquad \text{(A15)}$$